

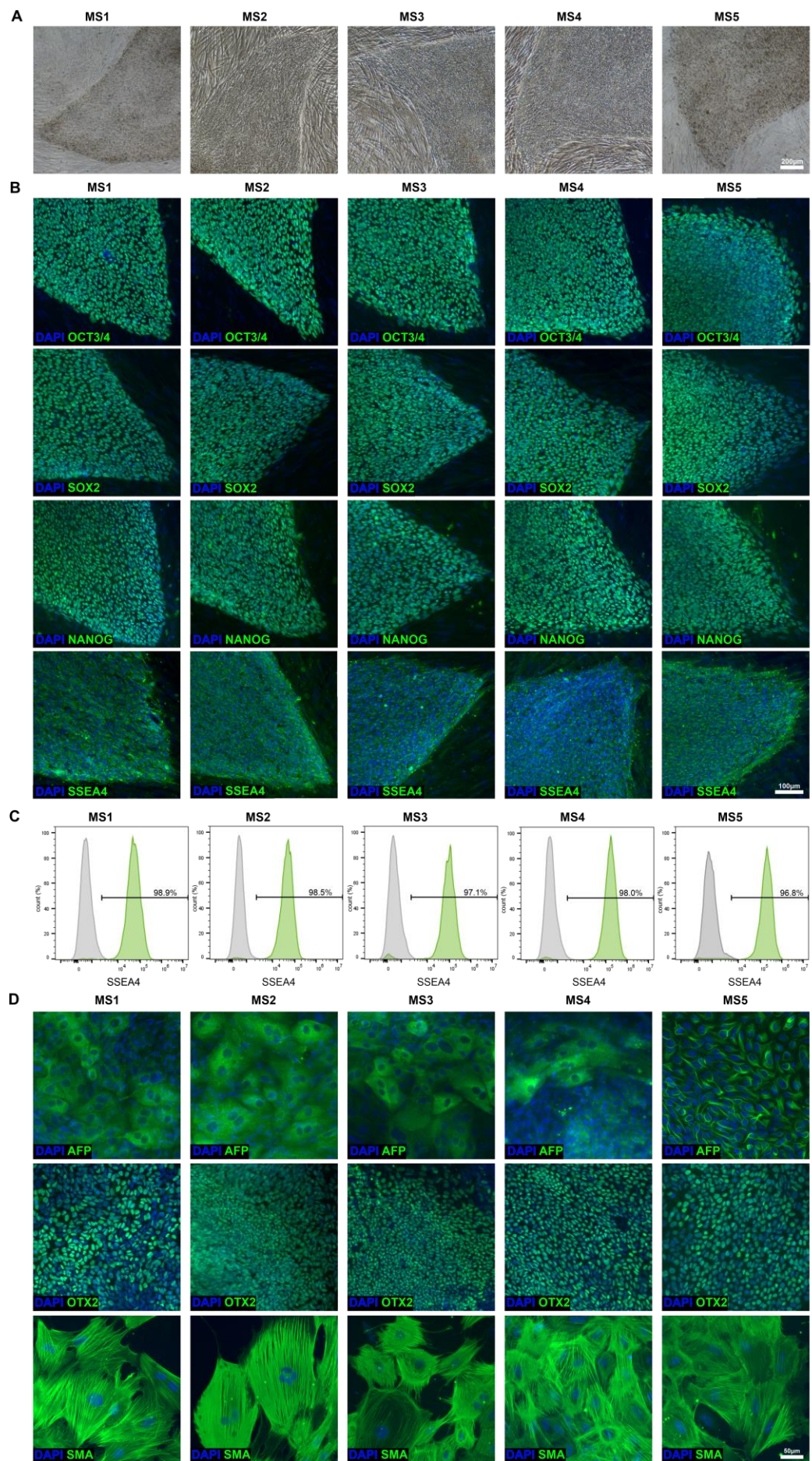
Supplementary information

Microglia from patients with multiple sclerosis display a cell-autonomous immune activation state

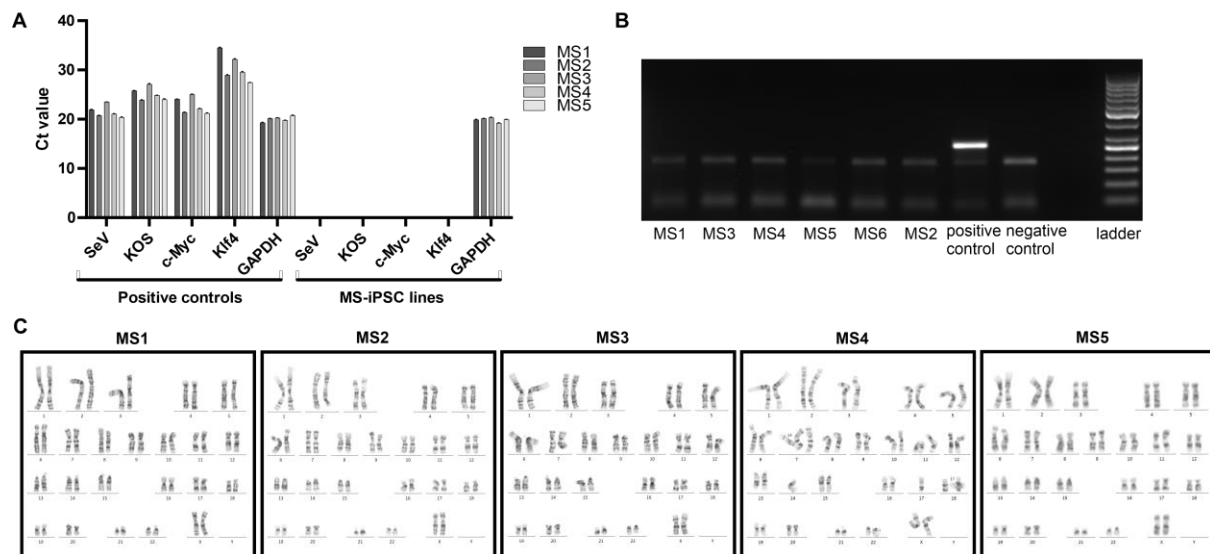
Tanja Hyvärinen^{1,†}, Johanna Tilvis^{1,†}, Luca Giudice², Iisa Tujula¹, Marjo Nylund^{3,4,5,6}, Sohvi Ohtonen², Flavia Scoyni^{2,7}, Henna Jäntti², Lassi Virtanen¹, Sara Pihlava¹, Roosa Kattelus¹, Heli Skottman⁸, Susanna Narkilahti⁹, Laura Airas^{3,4,5,6}, Tarja Malm², Sanna Hagman¹

[†]These authors contributed equally to this work.

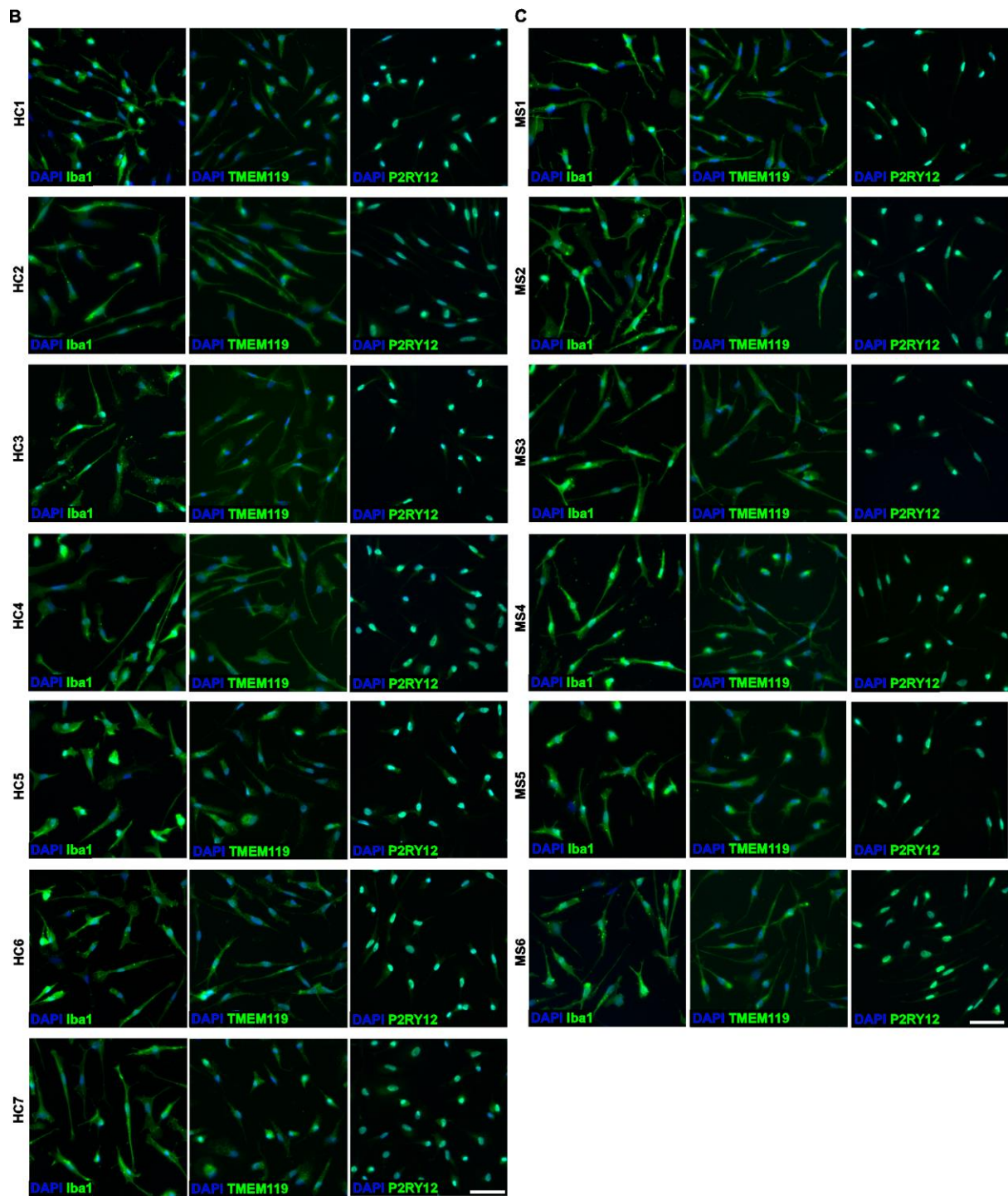
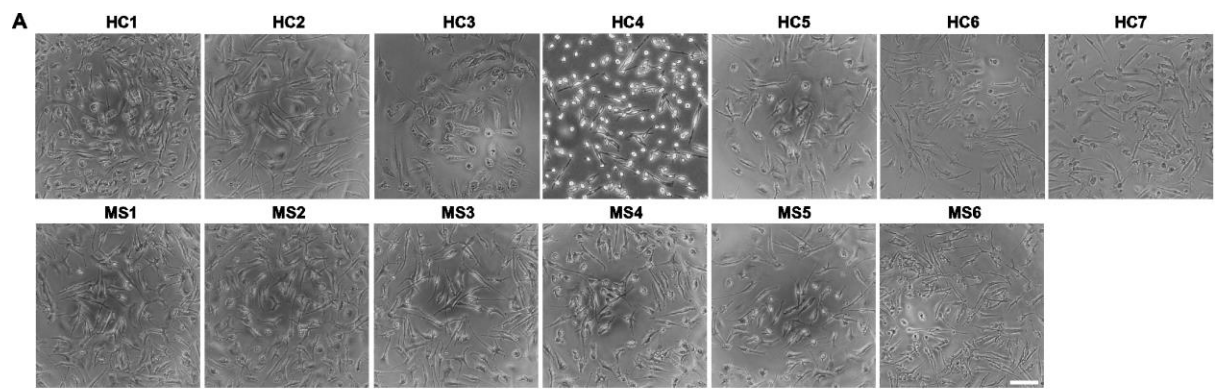
Supplementary Figures



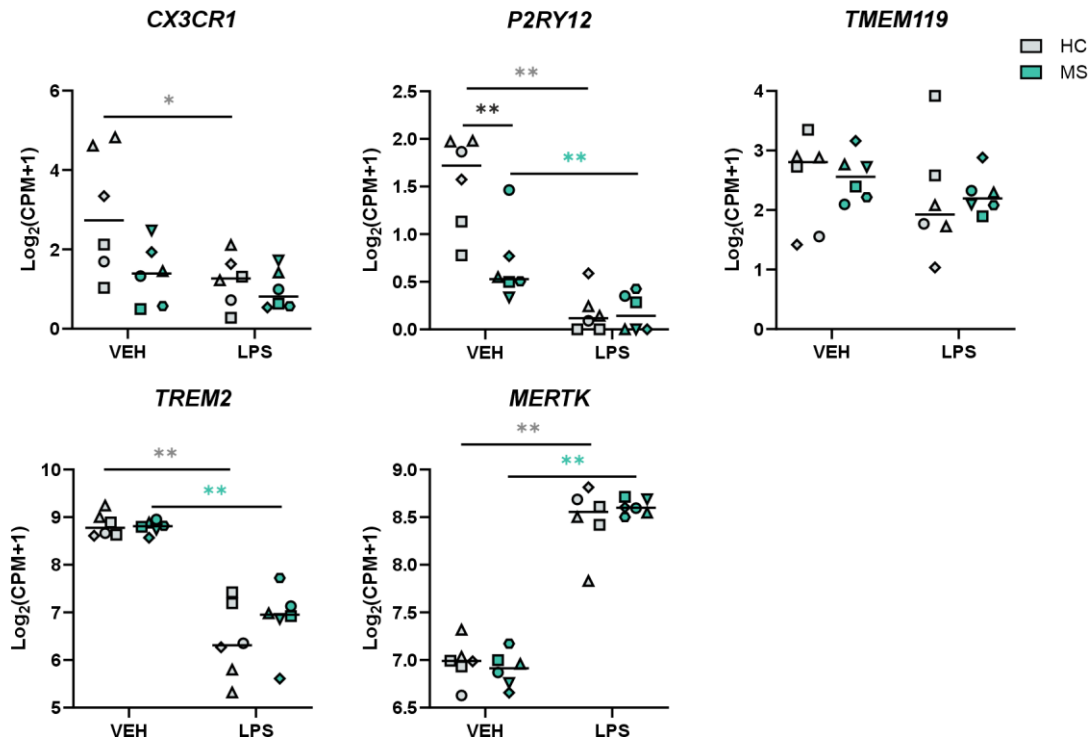
Supplementary Fig. 1 Characterization of the five MS patient-derived iPSC lines. **A** Representative phase contrast images and **B** images of immunofluorescence staining for OCT3/4, SOX2, NANOG and SSEA4. **C** Flow cytometry analysis of SSEA4 expression. **D** Representative images of AFP, OTX2 and SMA immunofluorescence staining confirmed the capacity of iPSCs to differentiate into the three germ layers *in vitro* through embryoid body formation.



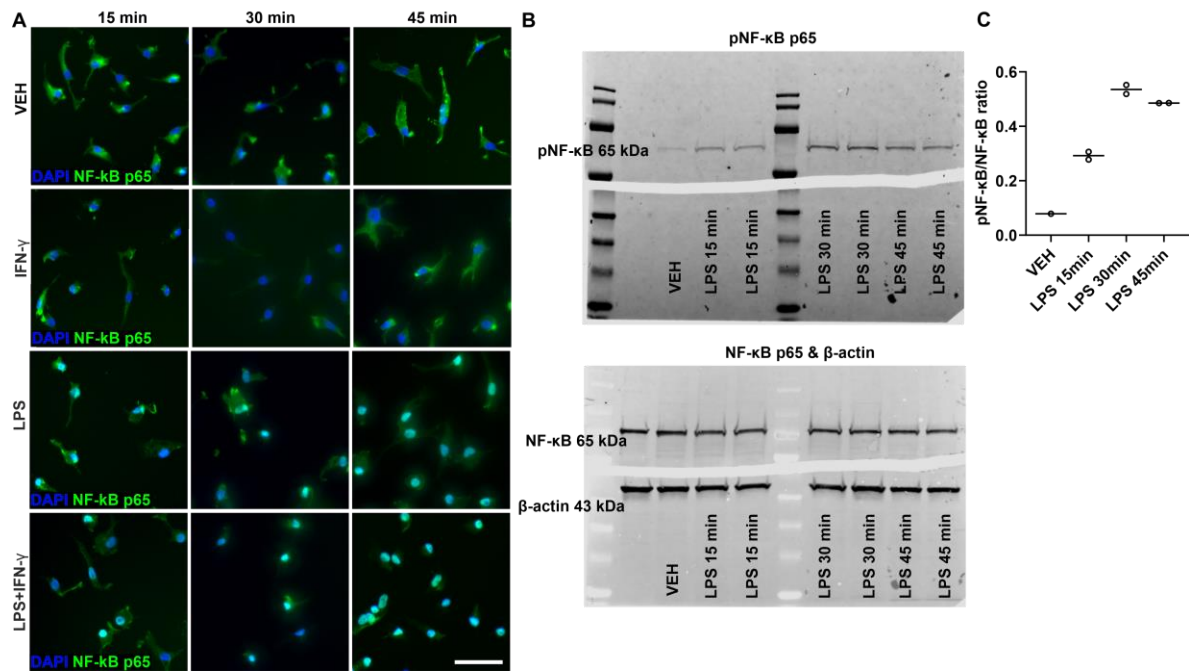
Supplementary Fig. 2 Characterization of MS patient-derived iPSC lines. **A** RT-qPCR analysis of the removal of Sendai virus vectors and transgenes (SeV, KOS, c-Myc and Klf4) from MS iPSCs. Positive controls were collected after transduction (passage 0), and MS-iPSC samples were collected at passage 7–10. **B** Cells were negative for mycoplasma detected via RT-PCR. **C** The karyotype analysis confirmed the normal diploid 46,XX karyotype.



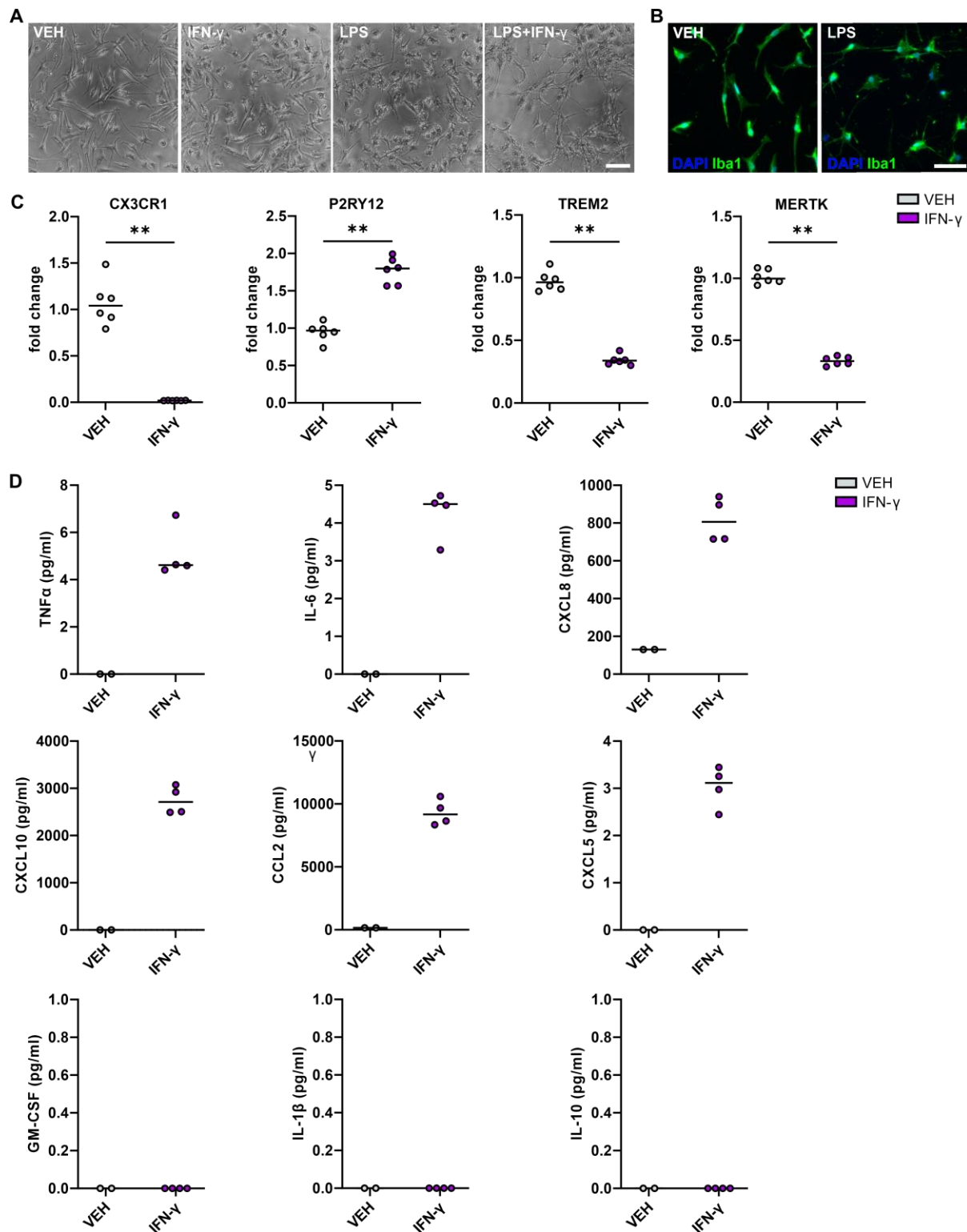
Supplementary Fig. 3 Characterization of HC and MS iPSC-derived iMGLs. **A** Representative phase contrast images of HC and MS iMGLs. Scale bar = 100 μ m. Representative images of immunofluorescence staining for Iba1, TMEM119 and P2RY12 in **B** HC and **C** MS iMGLs. Scale bar = 50 μ m.



Supplementary Fig. 4 Expression of microglial signature genes *CX3CR1*, *P2RY12*, *TMEM119*, *TREM2* and *MERTK* in RNA-sequencing data of vehicle- and LPS-stimulated HC and MS iMGLs. Data [$\log_2(\text{CPM}+1)$] presented as single datapoints and medians. $n = 6$, 4 HC cell lines and 6 MS cell lines, with 1-2 independent differentiations. Different symbols for individual iPSC lines are presented in Supplementary Table 1. Mann–Whitney U test, * $p < 0.05$, and ** $p < 0.01$.

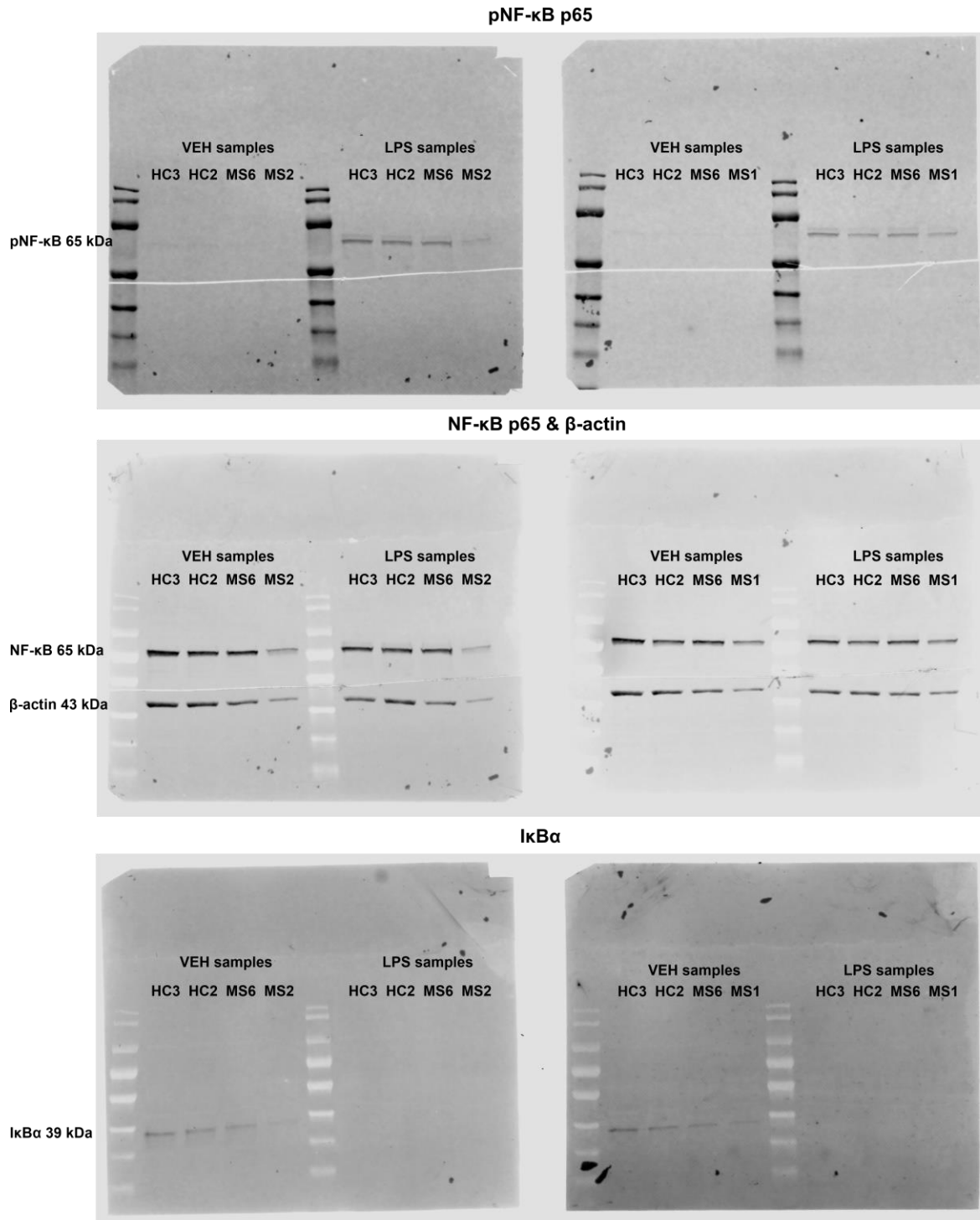


Supplementary Fig. 5 LPS stimulation activates the NF-κB signalling pathway in iMGLs. **A** Representative images of immunofluorescence staining for NF-κB p65 at 15 min, 30 min and 30 min in unstimulated, IFN γ -, LPS- or IFN γ +LPS-stimulated HC and MS iMGLs. Scale bar = 50 μm. **B** Western blots showing the levels of phospho-NF-κB p65, NF-κB p65 and β-actin in unstimulated sample and samples treated with LPS for 15 min, 30 min or 45 min. Nine micrograms of protein was loaded into each lane. **C** Quantification of the phospho-NF-κB p65 and NF-κB p65 expression ratios. Protein levels were normalized to those of β-actin. $n = 1-2$ technical replicates (wells), with 1 differentiation. The data presented as single datapoints and medians.



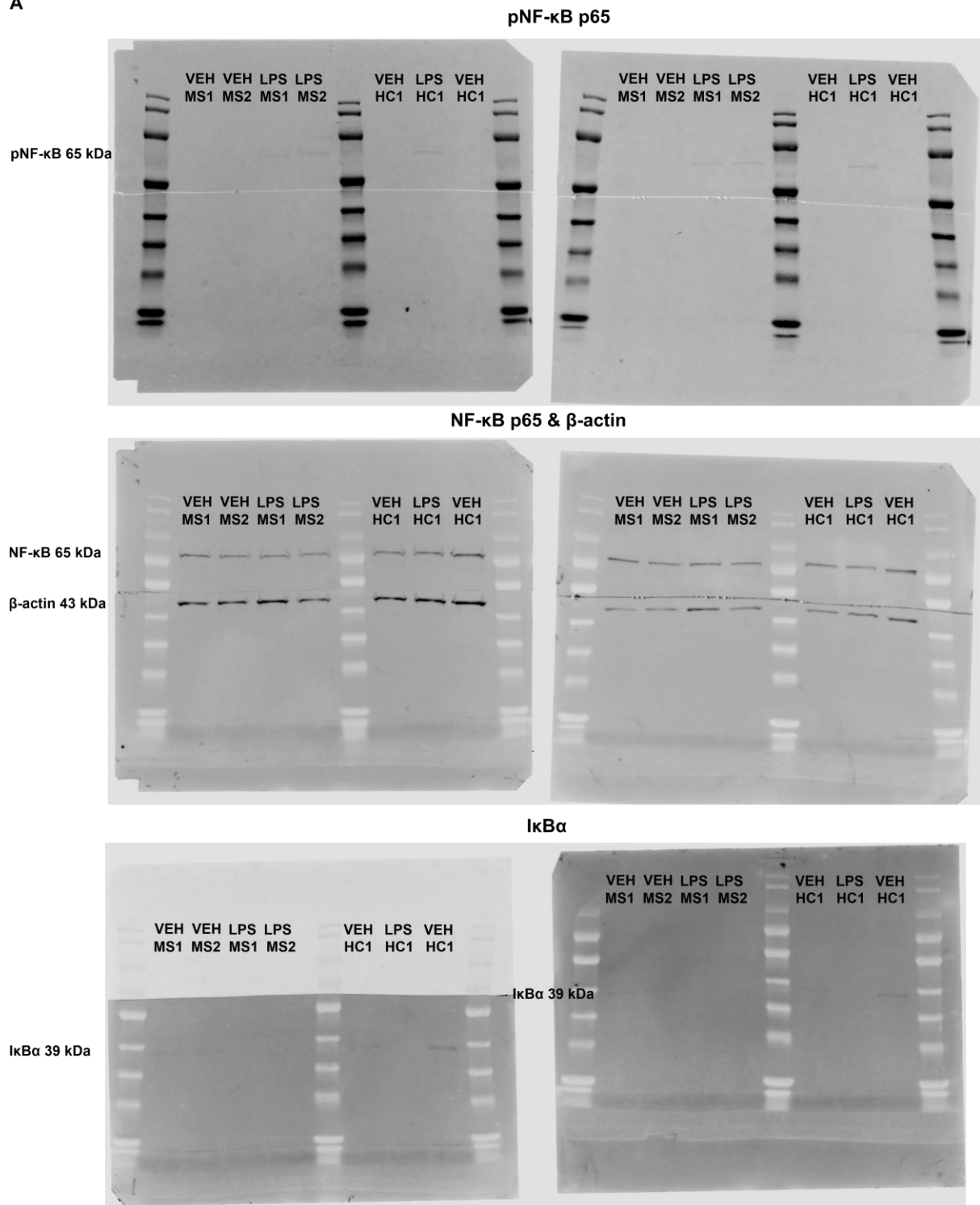
Supplementary Fig. 6 The effect of inflammatory stimulation on the iMGL phenotype. **A** Representative phase contrast images of vehicle- and IFN- γ -, LPS- or IFN- γ +LPS-stimulated iMGLs after 24 h of treatment. Scale bar = 100 μ m. **B** Representative images of Iba1 immunofluorescence staining in vehicle- and LPS-stimulated iMGLs after 24 h of treatment. Scale bar = 50 μ m. **C** qPCR analysis of the expression of the microglial signature genes

CX3CR1, *P2RY12*, *TREM2* and *MERTK* in vehicle- and IFN- γ -stimulated iMGLs after 24 h of treatment ($n = 6$ technical replicates, 1 HC cell line, with 1 differentiation). The data are presented as single data points and medians. **D** Analysis of cytokines secreted from vehicle- and IFN- γ -stimulated iMGLs after 24 h of treatment (1 HC cell line, with 1 differentiation). The data are presented as single data points and medians. Mann–Whitney U test, $**p < 0.01$.

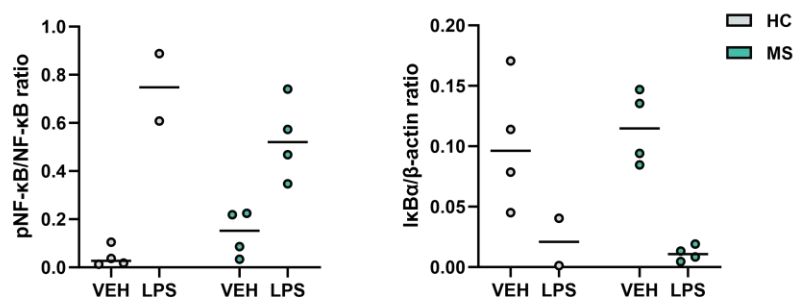


Supplementary Fig. 7 Western blots of NF- κ B signalling proteins in HC and MS iMGL samples. Western blots show the levels of phospho-NF- κ B p65, NF- κ B p65, β -actin and I κ B α in vehicle- and LPS-treated (45 min, 20 ng/ml) HC (2 cell lines) and MS iMGLs (3 cell lines); 1-2 technical replicates (wells), 1-2 independent differentiations. Nine micrograms of protein was loaded per lane. See also Figure 3D.

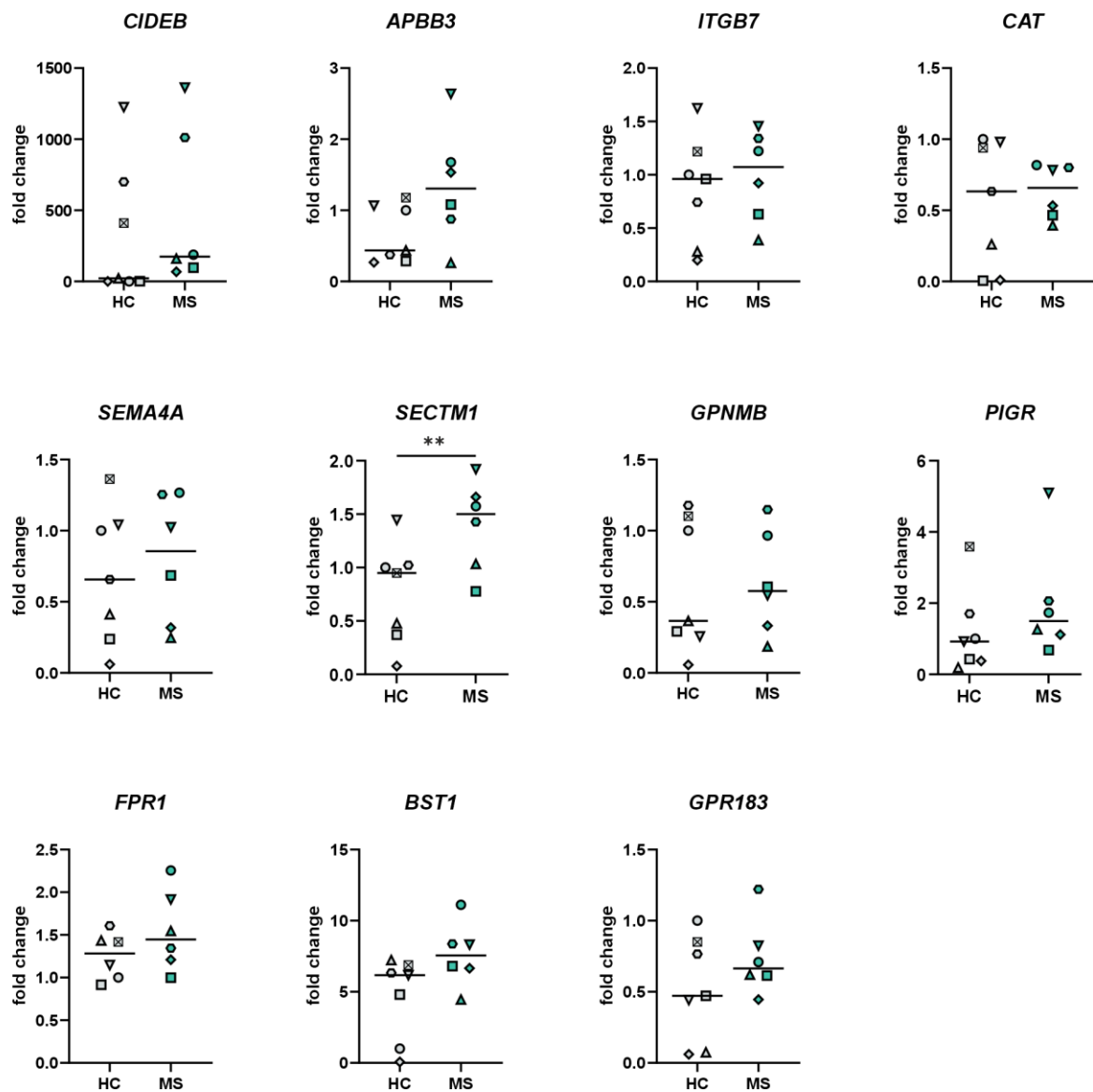
A



B

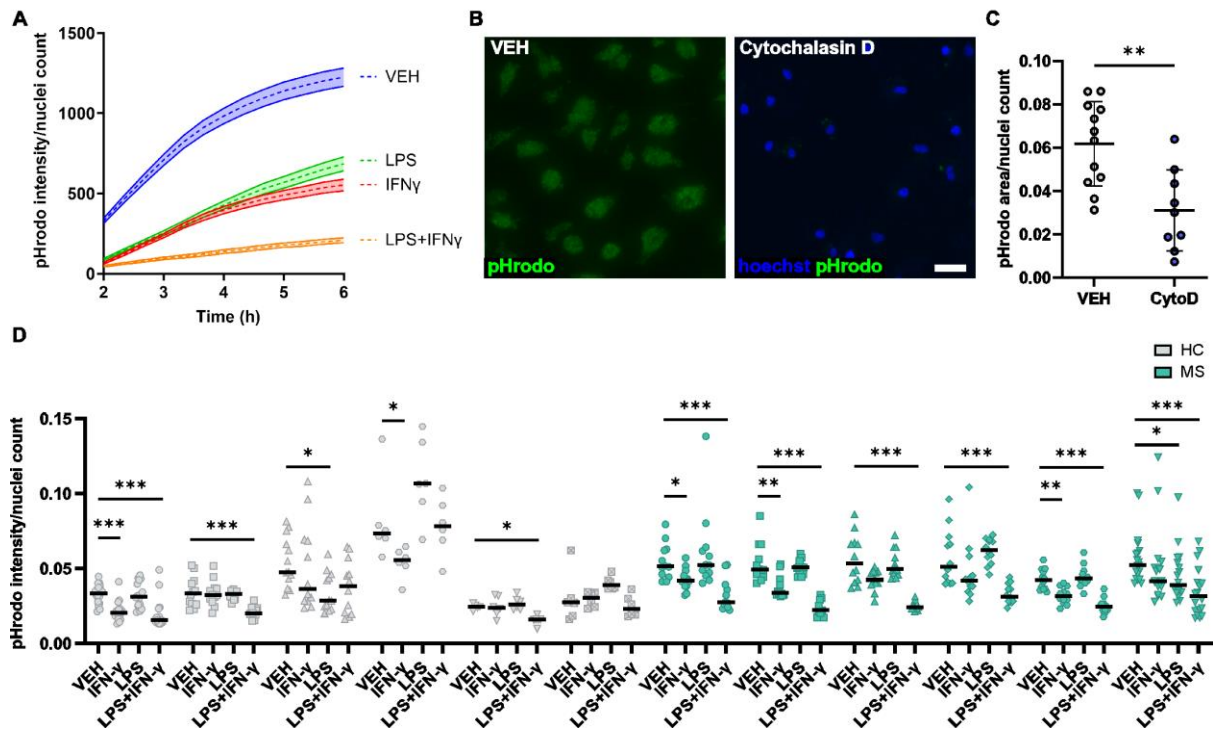


Supplementary Fig. 8 Western blots of NF- κ B signalling proteins in HC and MS iMGL samples. **A** Western blots show the levels of phospho-NF- κ B p65, NF- κ B p65, β -actin and I κ B α in vehicle- and LPS-treated (45 min, 20 ng/ml) HC (1 cell line, with 2 independent differentiations) and MS iMGLs (2 cell lines, with 1 differentiation). Five micrograms of protein was loaded per lane. **B** Quantification of the phospho-NF κ B p65 and NF κ B p65 expression ratios and I κ B α protein levels. Protein levels were normalized to those of β -actin. n = 2–4 samples, with 2 independent differentiations. The data are presented as single datapoints and medians.



Supplementary Fig. 9 Validation of RNA-seq results by qPCR analysis of selected genes in MS iMGLs compared to HC iMGLs. Fold change values for MS iMGL upregulated genes *CIDEB*, *APBB3*, *ITGB7*, *CAT*, *SEMA4A*, *SECTM1*, *GPNMB*, *PIGR*, *FPR1*, *BST1* and *GPR183*

in HC and MS iMGLs. $n = 6-7$, 7 HC cell lines and 6 MS cell lines. The data are presented as mean values for individual iPSC lines normalized to the HC1. Symbol coding for iPSC lines is shown in Supplementary Table 1. Mann–Whitney U test, $*p < 0.05$, and $**p < 0.01$.



Supplementary Fig. 10 Analysis of iMGL phagocytosis. **A** Representative time curve for the green fluorescence intensity of pHrodo zymosan phagocytosis in vehicle-, IFN- γ -, LPS- or IFN- γ +LPS-stimulated iMGLs after 24 h of treatment. $n = 18$ images per condition and time point; 6 wells/group, 1 differentiation. The data are presented as the means \pm SEMs. **B** Representative fluorescence images of pHrodo zymosan bioparticles phagocytosed by iMGLs treated with the vehicle or the phagocytosis inhibitor cytochalasin D for 2 h. Scale bar = 50 μ m. **C** Quantification of pHrodo zymosan phagocytosis in vehicle- and cytochalasin D-treated iMGLs. $n = 9-12$ images, 2–6 wells/group, with 2 independent differentiations. The data are presented as single data points and means \pm SD. Unpaired t test, $**p < 0.01$. **D** Quantification of pHrodo fluorescence intensity normalized to the number of nuclei for each 6 HC (grey colour) and 6 MS iMGL (green colour) cell line. $n = 5-19$ images per condition, with 1–3 differentiations per cell line. The data are presented as single data points and medians. The symbol coding of HC and MS iMGL cell lines is presented in Supplementary Table 1. Asterisks indicate statistically significant differences compared with the vehicle treatment within cell

lines, as determined using the Mann–Whitney U test with Bonferroni’s correction $*p < 0.05$, $**p < 0.01$, and $***p < 0.001$.

Supplementary Tables

Supplementary Table 1. Human induced pluripotent stem cell lines used in this study.

Symbol*	Cell line	Alias	Sex	Karyo-type	Health status	Origin	Reference
●	MS1	MS1	F	46,XX	MS	PBMC	this article
■	MS2	MS2	F	46,XX	MS	PBMC	this article
▲	MS3	MS3	F	46,XX	MS	PBMC	this article
◆	MS4	MS4	F	46,XX	MS	PBMC	this article
●	MS5	MS5	F	46,XX	MS	PBMC	this article
▼	MS6	MS6	F	46,XX	MS	PBMC	Lotila et al. 2022 [1]
○	UTA.04511.WT	HC1	M	46,XY	Healthy	Fibroblast	Ojala et al. 2016 [2]
□	UTA.10902.EURCCs	HC2	F	46,XX	Healthy	Fibroblast	Hongisto et al. 2017 [3]
△	UTA.04602.WT	HC3	F	46,XX	Healthy	Fibroblast	Ojala et al. 2016 [2]
◇	UTA.11311.EURCCs	HC4	F	46,XX	Healthy	Fibroblast	Häkli et al. 2022 [4]
⬡	Hel54.1	HC5	F	46,XX	Healthy	PBMC	Trokovic et al. 2014 [5]
▽	Hel55.5	HC6	F	46,XX	Healthy	PBMC	Trokovic et al. 2014 [5]
⊠	Hel96.6	HC7	F	46,XX	Healthy	PBMC	Trokovic et al. 2014 [5]

Abbreviations: HC, healthy control; MS, multiple sclerosis; F female; M male; PBMC peripheral mononuclear cells.

*Symbols indicate the iPSC lines used in the figures.

Supplementary Table 2. qPCR primers used to characterize iMGLs.

Target	Cat no.	Supplier
<i>APBB3</i>	Hs00195923_m1	Thermo Fisher Scientific
<i>BST1</i>	Hs01070189_m1	Thermo Fisher Scientific
<i>CAT</i>	Hs00156308_m1	Thermo Fisher Scientific
<i>CD74</i>	Hs00269961_m1	Thermo Fisher Scientific
<i>CIDEA</i>	Hs00205339_m1	Thermo Fisher Scientific
<i>CX3CR1</i>	Hs04187059_m1	Thermo Fisher Scientific
<i>FPR1</i>	Hs00181830_m1	Thermo Fisher Scientific
<i>GPNMB</i>	Hs01095669_m1	Thermo Fisher Scientific
<i>GPR183</i>	Hs00953886_m1	Thermo Fisher Scientific
<i>HLA-DPA1</i>	Hs00410276_m1	Thermo Fisher Scientific
<i>HLA-DRA</i>	Hs00219575_m1	Thermo Fisher Scientific
<i>HLA-DRB1</i>	Hs04192464_mH	Thermo Fisher Scientific
<i>ITGB7</i>	Hs01565750_m1	Thermo Fisher Scientific
<i>MERTK</i>	Hs01031979_m1	Thermo Fisher Scientific
<i>P2RY12</i>	Hs00224470_m1	Thermo Fisher Scientific
<i>PIGR</i>	Hs00922561_m1	Thermo Fisher Scientific
<i>SECTM1</i>	Hs00356334_m1	Thermo Fisher Scientific
<i>SEMA4A</i>	Hs00223617_m1	Thermo Fisher Scientific
<i>TMEM119</i>	Hs01938722_u1	Thermo Fisher Scientific
<i>TREM2</i>	Hs00219132_m1	Thermo Fisher Scientific

References

- [1] Lotila J, Hyvärinen T, Skottman H, Airas L, Narkilahti S, Hagman S. Establishment of a human induced pluripotent stem cell line (TAUi008-A) derived from a multiple sclerosis patient. *Stem Cell Research* 2022;63:102865. <https://doi.org/10.1016/j.scr.2022.102865>.
- [2] Ojala M, Prajapati C, Pölönen R-P, Rajala K, Pekkanen-Mattila M, Rasku J, et al. Mutation-Specific Phenotypes in hiPSC-Derived Cardiomyocytes Carrying Either Myosin-Binding Protein C Or α -Tropomyosin Mutation for Hypertrophic Cardiomyopathy. *Stem Cells International* 2016;2016:1684792.
- [3] Hongisto H, Ilmarinen T, Vattulainen M, Mikhailova A, Skottman H. Xeno- and feeder-free differentiation of human pluripotent stem cells to two distinct ocular epithelial cell types using simple modifications of one method. *Stem Cell Res Ther* 2017;8:291. <https://doi.org/10.1186/s13287-017-0738-4>.
- [4] Häkli M, Kreutzer J, Mäki A-J, Välimäki H, Cherian RM, Kallio P, et al. Electrophysiological Changes of Human-Induced Pluripotent Stem Cell-Derived Cardiomyocytes during Acute Hypoxia and Reoxygenation. *Stem Cells Int* 2022;2022:9438281. <https://doi.org/10.1155/2022/9438281>.
- [5] Trokovic R, Weltner J, Nishimura K, Ohtaka M, Nakanishi M, Salomaa V, et al. Advanced Feeder-Free Generation of Induced Pluripotent Stem Cells Directly From Blood Cells. *Stem Cells Transl Med* 2014;3:1402–9. <https://doi.org/10.5966/sctm.2014-0113>.